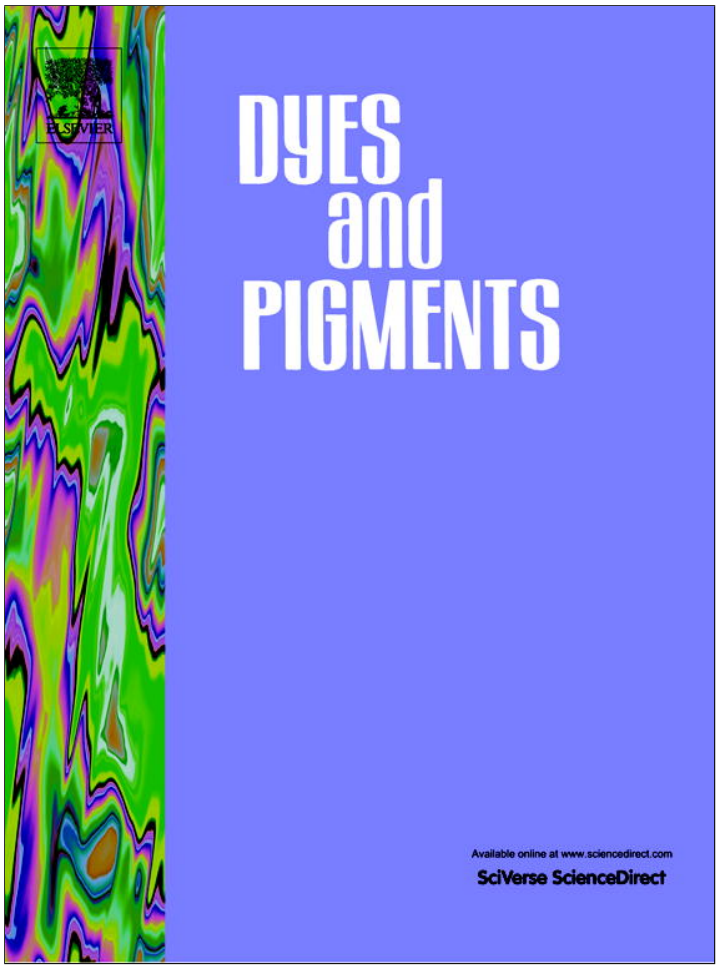

(This is a sample cover image for this issue. The actual cover is not yet available at this time.)

Dyes and Pigments 96 (2013) 626–635

Contents lists available at SciVerse ScienceDirect

Dyes and Pigments

journal homepage: www.elsevier.com/locate/dyepig

Photophysics and photobiology of novel liposomal formulations of 2,9(10),16(17),23(24)-tetrakis[(2-dimethylamino)ethylsulfanyl]phthalocyaninatozinc(II)

Noelia C. López Zeballos [a], Julieta Marino [b], María C. García Vior [c], Nicolás Chiarante [b], Leonor P. Roguin [b], Josefina Awruch [c,*], Lelia E. Dicelio [a]

[a] INQUIMAE, Departamento de Química Inorgánica, Analítica y Química Física, Facultad de Ciencias Exactas y Naturales, Universidad de Buenos Aires, Ciudad Universitaria, Pabellón II, 1428 Buenos Aires, Argentina
[b] Instituto de Química y Fisicoquímica Biológicas (UBA-CONICET), Facultad de Farmacia y Bioquímica, Junín 956, 1113 Buenos Aires, Argentina
[c] Departamento de Química Orgánica, Facultad de Farmacia y Bioquímica, Universidad de Buenos Aires, Junín 956, 1113 Buenos Aires, Argentina

ARTICLE INFO

Article history:
Received 18 June 2012
Received in revised form
25 September 2012
Accepted 5 November 2012
Available online 15 November 2012

Keywords:
Photodynamic therapy
Phthalocyanine
Liposome
Singlet oxygen
Photocytotoxicity
KB cells

ABSTRACT

Six novel liposomal formulations of 2,9(10),16(17),23(24)-tetrakis[(2-dimethylamino)ethylsulfanyl]phthalocyaninatozinc(II) (Pc9) were investigated to establish how the environments affect their photophysical and photobiological properties. The incorporation efficiency and solubility during a time period were evaluated. All Pc9-liposomal formulations were efficient singlet oxygen quantum yield generators. The photobiological potentials were evaluated on human nasopharynx KB carcinoma cells. None of the formulations studied showed cytotoxic effects in the absence of light, whereas all of them showed good performance after irradiation. The 50% inhibition of cell proliferation (IC_{50}) was in the range of 0.21–0.47 μM for Pc9-loaded liposome formulations. A lysosomal localization was found for S-PEG as well as for S.

1. Introduction

Photodynamic therapy (PDT) involves the generation of highly reactive species capable of destroying cancer tissues. The reactive species are generated by the irradiation of a photosensitizer with visible light in the presence of oxygen [1,2].

Phthalocyanines have been found to be useful photosensitizers for PDT [3–6]. Since phthalocyanines are highly hydrophobic, which make it difficult to administer them parenterally in physiological media, delivery strategies have been developed to increase their solubility [7–9]. Moreover, the tendency of phthalocyanines to aggregate has a strong negative effect on their photophysical properties [10].

Nanocarriers, such as liposomes, micelles, nanoemulsions, polymeric nanoparticles and many others, are widely used as carrier systems for water-insoluble drugs in pharmaceutics [11].

In particular, liposomes with various lipid compositions have been reported as carrier systems for water insoluble phthalocyanines [12,13].

We have recently studied the photophysical properties, size and stability of different formulations of liposomes containing the lipophilic 2,9(10),16(17),23(24)-tetrakis(1-adamantylsulfanyl)phthalocyaninatozinc(II). These formulations revealed to be efficient singlet molecular oxygen generators [13].

Since 2,9(10),16(17),23(24)-tetrakis[(2-dimethylamino)ethylsulfanyl]phthalocyaninatozinc(II) (Pc9) exhibits a better liposomal incorporation than the above-mentioned phthalocyanine, further studies have been initiated to investigate the photophysical parameters of Pc9 incorporated into these lipid environments. In addition, its photobiological properties were evaluated on human nasopharynx KB carcinoma cells.

2. Materials and methods

2.1. Materials

2,9(10),16(17),23(24)-tetrakis[(2-dimethylamino)ethylsulfanyl]phthalocyaninatozinc(II) (Pc9) [14] (Fig. 1) and tetra-*t*-butyl phthalocyaninatozinc(II) [15] were synthesized in our laboratory. L-α-Phosphatidylethanolamine from egg yolk Type III (PEEY); L-α-Phosphatidylcholine from egg yolk, Type XVI-E (PCEY); 1,2-Distearoyl-*sn*-

* Corresponding author. Tel.: +54 11 4964 8252; fax: +54 11 4508 3645.
E-mail address: jawruch@ffyb.uba.ar (J. Awruch).

0143-7208/$ – see front matter © 2012 Elsevier Ltd. All rights reserved.
http://dx.doi.org/10.1016/j.dyepig.2012.11.005

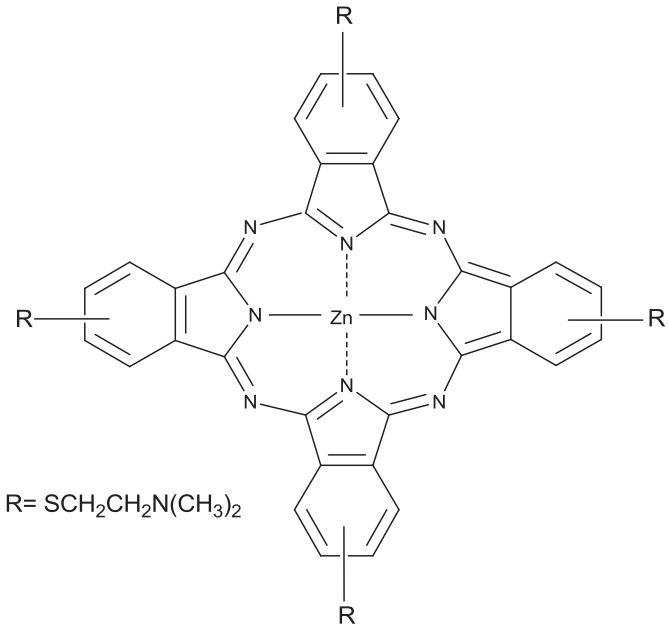

Fig. 1. Chemical structure of phthalocyanine (Pc9).

glycero-3-phosphoethanolamine (DSPE); L-α-Phosphatidylethanolamine distearoyl methoxypolyethylene glycol conjugate (DSPE-PEG); 1,2-Dipalmitoyl-*sn*-glycero-3-phosphocholine (DPPC); Cholesterol BioReagent suitable for cell culture (CHOL); HEPES BioUltra for molecular biology; 2′,7′-dichlorofluorescein-diacetate (DCFH-DA) and 3-(4,5-Dimethylthiazol-2-yl)-2,5-diphenyltetrazolium bromide (MTT) were purchased from Sigma–Aldrich Germany (Schnelldorf, Germany). LysoTracker Green DND-26 and MitoTracker Green FM were obtained from Invitrogen (Carisbad, CA, USA). Sodium chloride was obtained from Mallinckrodt (Phillipsburg, NJ, USA). Imidazole BioUltra and Methylene Blue Hydrate (MB) were from Fluka (Sigma–Aldrich, India); N,N-Diethyl-4-nitrosoaniline 97% and Tetrahydrofuran (THF) spectrophotometric grade were from Sigma–Aldrich (Steinheim, Germany). Diethyl ether was from Carlo Erba (Rodano, Italy), and Chloroform from Merck-Química Argentina (Buenos Aires, Argentina). All chemicals were of reagent grade and used without further purification. Distilled water treated in a Milli-Q system (Millipore) was used.

2.2. Instrumentation

Electronic absorption spectra were determined with a Shimadzu UV-3101 PC spectrophotometer and fluorescence spectra were monitored with a QuantaMaster Model QM-1 PTI spectrofluorometer. pH was measured with a Thermo pH meter Altronix TPX-1. Static light scattering (SLS) experiments were carried out using an SLS 90 Plus/BI-MAS (MultiAngle Particle Sizing Option) equipped with a He–Ne laser operating at 632.8 nm and 15 mW. The sonicator used was MSE Soniprep 150.

2.3. Preparation of unilamellar liposomes

The preparation of unilamellar liposomes was achieved as described elsewhere [13] (See Table 1).

2.4. Sample preparation. Determination of incorporation efficiency (IE)

Stock solutions of Pc9 were prepared in THF, kept at 4 °C, and carefully protected from ambient light. The dye and carrier concentrations are indicated in each experiment.

Table 1
Liposomal composition and Pc9 incorporation efficiency (IE).

Liposome type	Lipid composition	Molar relation	[a]IE (%)
D1	DPPC: CHOL	24:1	83.5 ± 1.1
D2	DPPC	1	92.5 ± 2.1
M1	PCEY: PEEY: CHOL	16:16:1	82.9 ± 8.6
M2	PCEY: PEEY	1:1	88.8 ± 2.9
S	DPPC: PCEY: PEEY: DSPE: CHOL	1:8:7:1:3	90.5 ± 10.0
S-PEG	DPPC: PCEY: PEEY: DSPE-PEG: CHOL	1:8:7:1:3	74.7 ± 0.1

[a] Data represent the mean value ± standard error of three independent experiments.

Liposomes with Pc9 incorporated were disrupted using Triton-X 100 to fully release the dye incorporated into the liposomes, and the absorbance of samples measured after leaving them at room temperature for 24 h. The absorbance of Pc9 at λ_{max} indicated in Table 2 for each sample was measured to determine the concentration of Pc9 incorporated. The IE was calculated by equation (1)

$$IE = \frac{[\text{Incorporated ZnPc}]}{[\text{Initial ZnPc loaded}]} \times 100 \quad (1)$$

2.5. Photophysical properties

2.5.1. Spectroscopic studies

Absorption and emission spectra were recorded with a 10 × 10 mm quartz cuvette with a 500 μL capacity at room temperature.

Emission spectra of Pc9 were recorded at an excitation wavelength (λ_{exc}) of 610 nm (Q-band) between 630 and 800 nm; a cut-off filter was used to prevent the excitation beam from reaching the detector (Schott RG 630).

Emission and absorption spectra of liposomal phthalocyanines were corrected for light scattering by subtracting the spectra from empty liposomes.

Spectroscopic experiments were carried out at concentrations 1×10^{-4} M.

2.5.2. Fluorescence quantum yields

Fluorescence quantum yields (Φ_F) were determined by comparing them with those of tetra-*t*-butyl phthalocyaninato-zinc(II) ($\Phi_F = 0.30$ in toluene) as a reference at an λ_{exc} of 610 nm and calculated as described elsewhere [15].

2.5.3. Quantum yield of singlet oxygen production

The quantum yield of singlet oxygen generation rates (Φ_Δ) was determined using standard chemical monitor bleaching rates [16]. Imidazol (8 mM) and *N*,*N*-diethyl-4-nitrosoaniline (40–50 μM) in HEPES was used for Pc9-loaded liposomes [17]. *N*,*N*-diethyl-4-nitrosoaniline decay was monitored at 440 nm.

A projector lamp (Philips 7748SEHJ, 24 V–250 W) and a cut-off filter at 610 nm (Schott, RG 610) were used to generate polychromatic irradiation and a water filter to prevent infrared radiation. The liposomal samples of Pc9 and the reference (MB: $\Phi_\Delta = 0.56$ in buffer) [16] were irradiated within the same wavelength interval λ_1–λ_2, and Φ_Δ was calculated according to Amore et al. [18].

2.5.4. Aggregation studies of Pc9 in liposomal formulations

The intensity absorption ratio of the two bands corresponding to the monomer and oligomers was calculated. The higher values of the ratio indicated a disaggregated dye form [19,20]. This ratio was calculated for all liposomal formulations using the λ_{max} indicated in Table 2. These values were compared with those obtained in THF, where aggregation was not observed, and with those obtained in HEPES pH 7.4 and 145 mM NaCl.

Table 2
Photophysical parameters of Pc9 in homogeneous media and inside liposomes.

Photophysical parameters	THF	D1	D2	M1	M2	S	S-PEG
[b]Φ_Δ	0.60 ± 0.07	0.34 ± 0.06	0.42 ± 0.07	0.51 ± 0.08	0.33 ± 0.05	0.37 ± 0.10	0.34 ± 0.10
[b]Φ_F	0.280 ± 0.036	0.007 ± 0.001	0.008 ± 0.001	0.004 ± 0.001	0.019 ± 0.003	0.024 ± 0.006	0.004 ± 0.001
$\lambda_{max\ absorb}$ (nm)	688	646.5–693[a]	642.5–687[a]	644–694.5[a]	656.5–705.2[a]	647.5–692.5[a]	649-693.5[a]
$\lambda_{max\ emission}$ (nm)	694	699	699	700	698	699	699
Intensity absorption rate	6.09	0.95	0.81	0.76	1.55	1.20	1.07

[a] Absorption corresponding to monomer and oligomer species.
[b] Data represent the mean value ± standard error of three independent experiments.

2.6. Determination of Pc9 solubility in liposomes

Different concentrations of Pc9 (1, 2, 4, 8, and 16 μM) were used for each lipid formulation. Fluorescence intensities were measured at λ_{max} at predetermined intervals of 1, 2, 7, 15, and 30 days. To evaluate the amount of Pc9 incorporated into the liposomes, the fluorescence values obtained were interpolated in a calibration curve covering the range between 1 and 16 μM (with a correlation factor of 0.9571). Solvent was used as blank. Experiments were carried out in duplicate and concentrations are expressed in μM. The intrinsic solubility (S_0) of Pc9 in different liposomes was defined as the highest concentration measured for any of the formulations on day 30 [21].

2.7. Binding experiments

Fluorescence measurements were carried out at a fixed amount of Pc9 (81.24 μM) and increasing concentrations of liposome from 0 to 260 μg/mL. As Pc9 is insoluble in aqueous solution, the incorporation of the dye can be represented as:

$$F - F_0 = (F_\infty - F_0) \times \frac{[L_x]}{(1/K_a) + [L_x]} \quad (2)$$

where K_a is the equilibrium binding constant between the aqueous-phase dispersed aggregates and membrane-bound monomers, $(F-F_0)/(F_\infty-F_0)$ is the fraction of Pc9 associated to L_x as monomer, F is the maximum of each emission spectrum, and F_0 and F_∞ are the fluorescence in the absence and at maximum association to L_x [10].

2.8. Biological studies

2.8.1. Cells and culture conditions

Human nasopharynx carcinoma KB cells (ATCC CCL-17) were maintained in Minimum Essential Medium (MEM, Gibco BRL) containing 10% (v/v) fetal bovine serum (FBS, Gibco BRL), 2 mM L-glutamine, 50 U/mL penicillin, 50 μg/mL streptomycin, 1 mM

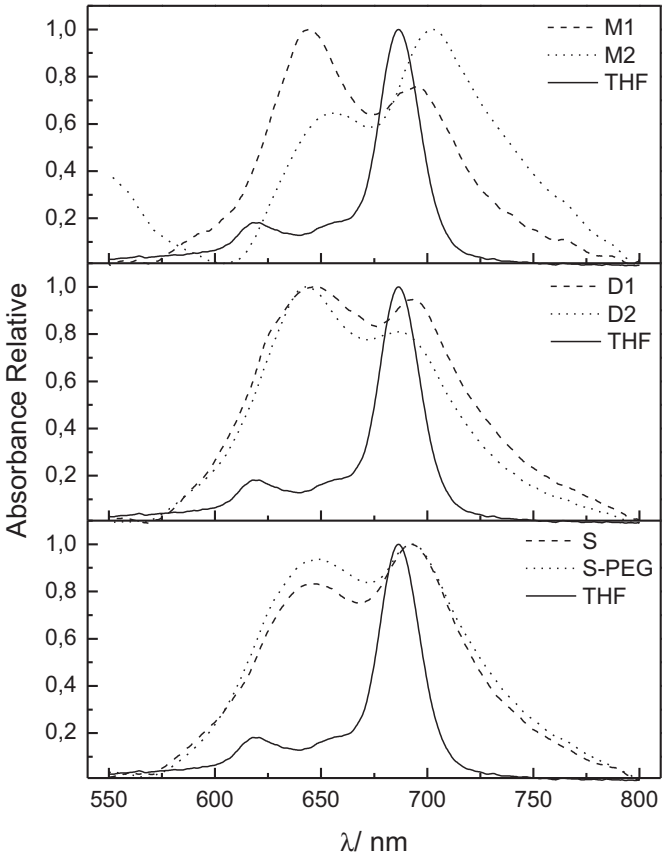

Fig. 2. Absorption spectra of Pc9 in a homogeneous medium (THF) and inside liposomes.

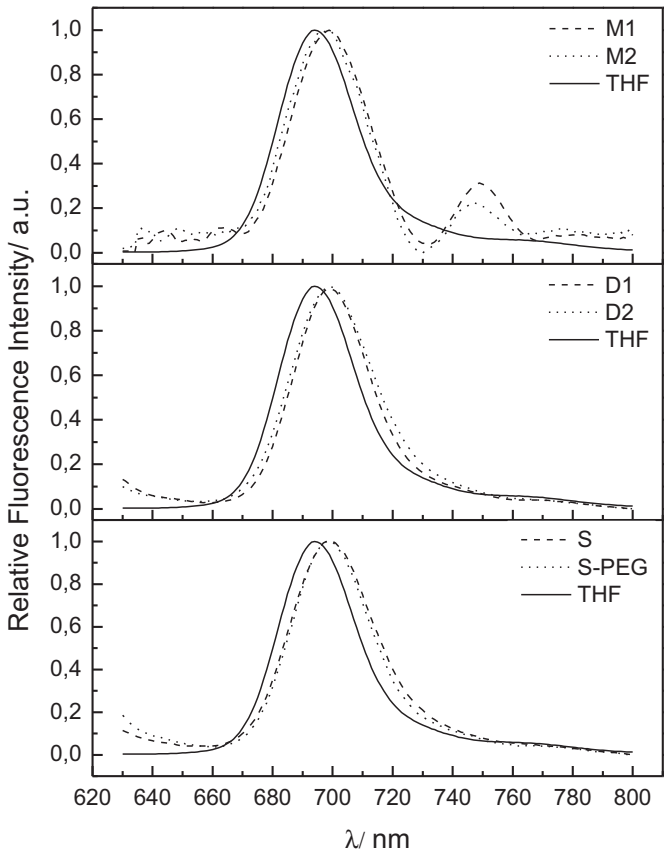

Fig. 3. Emission spectra of Pc9 at different liposomal formulations at λ_{exc} = 610 nm.

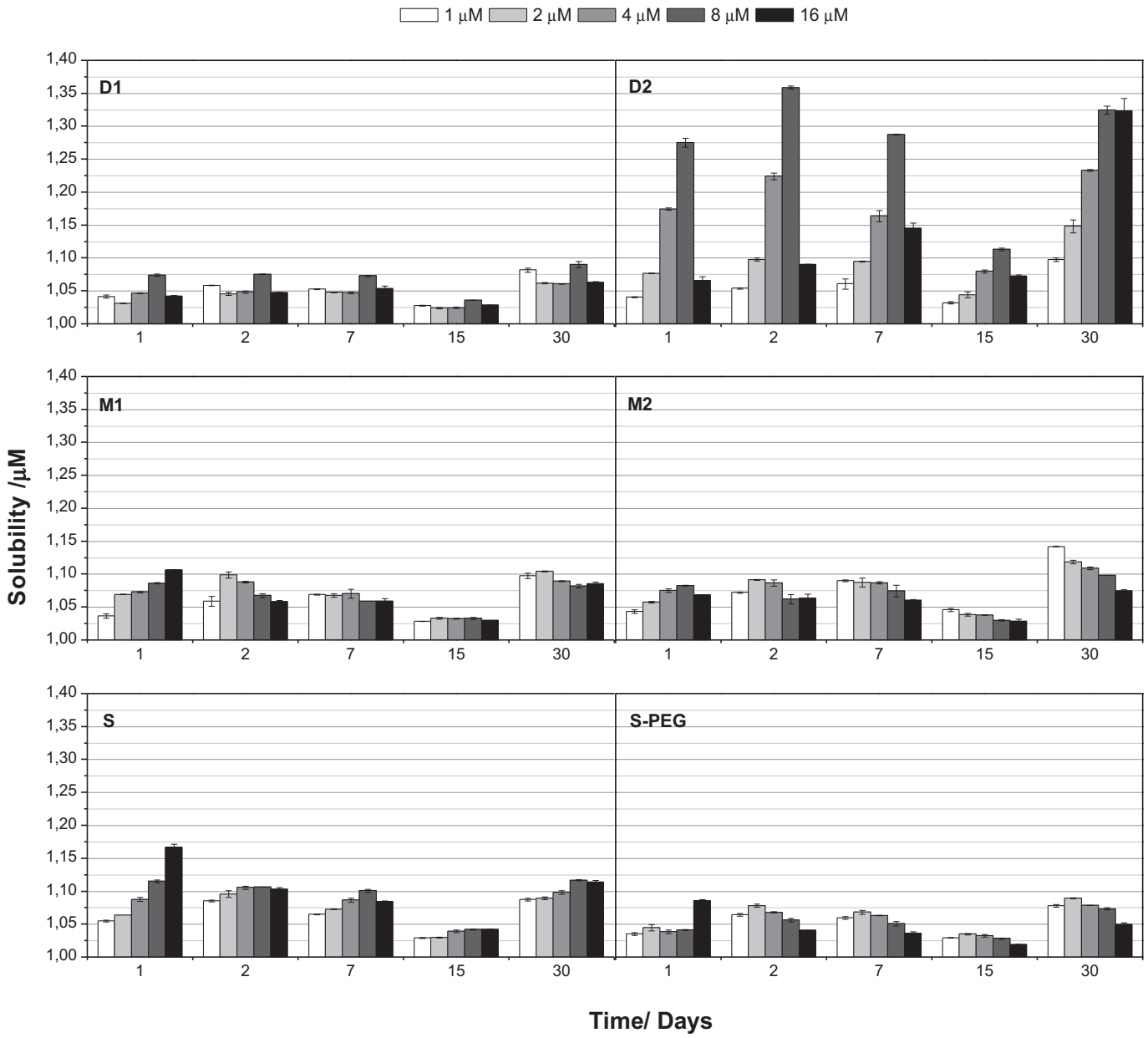

Fig. 4. Solubility of Pc9 in different liposomes over one month.

sodium pyruvate and 4 mM sodium bicarbonate, in a humidified atmosphere of 5% CO_2 at 37 °C.

2.8.2. Dark cytotoxicity and photocytotoxicity

KB cells were plated at a density of 1×10^4 cells/well in 96-well microplates and incubated overnight at 37 °C until 70–80% of confluence. Then, the culture medium was replaced by MEM containing 4% FBS and different concentrations of empty or Pc9-loaded liposomes. After 24 h, compounds were removed and cells were exposed to a light dose of 2.8 J cm^{-2}, 1.17 mW cm^{-2}, with a 150 W halogen lamp equipped with a 10 mm water filter to maintain cells cool and attenuate IR radiation. In addition, a cut-off filter was used to bar wavelengths shorter than 630 nm, as described previously [14]. In parallel, non-irradiated cells were used to study dark cytotoxicity. Following treatment, cells were incubated for an additional 24 h period and cell viability was determined by the MTT reduction assay. The absorbance (595 nm) was measured in a Biotrack II Microplate Reader (Amersham Biosciences).

2.8.3. Intracellular production of reactive oxygen species (ROS)

The endogenous ROS content was measured by using the probe DCFH-DA. Briefly, KB cells were plated at a density of 6×10^4 cells/

Table 3
Association constants of Pc9 into liposomes.

Liposome type	K_a (μg/mL)$^{-1}$
D1	1.84×10^{-2}
D2	1.96×10^{-2}
M1	0.62×10^{-2}
M2	1.96×10^{-2}
S	0.95×10^{-2}
S-PEG	3.99×10^{-2}

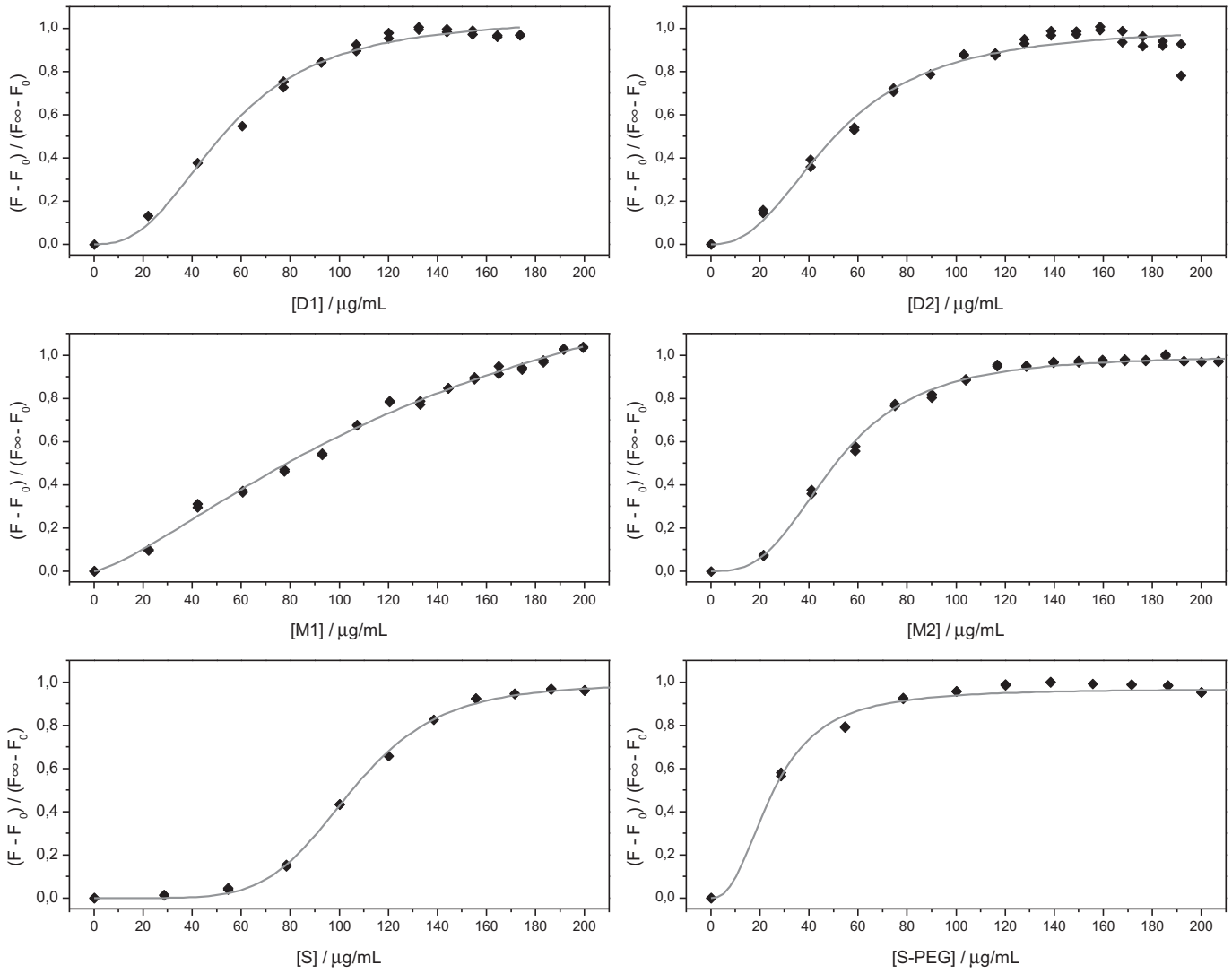

Fig. 5. Association of Pc9 into liposomes. $T = 20\ ^{\circ}C$, $\lambda_{exc} = 610$ nm.

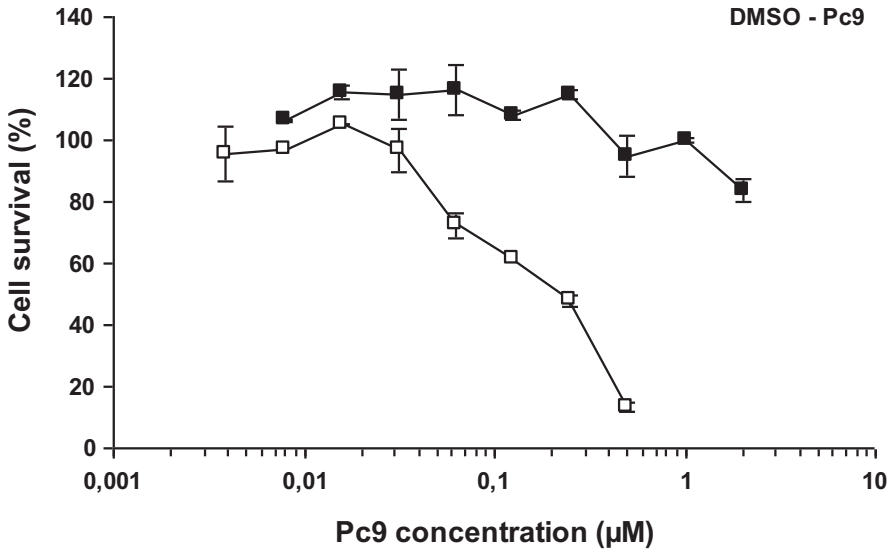

Fig. 6. Effect of Pc9 on KB cell viability. Different concentrations of Pc9 were incubated with KB cells in the dark (■) or exposed to a light dose of 2.8 J cm^{-2} (□). The MTT cytotoxicity assay was carried out 24 h after the treatment, as described under Materials and methods. Results are expressed as the percentage of cell growth obtained in the absence of Pc9 (control) and represent the mean ± S.E. of three different experiments.

well in 24-well microplates and incubated overnight at 37 °C until 70–80% of confluence. Then, the culture medium was replaced by MEM containing 4% FBS and 1 μM of Pc9 incorporated in different liposomal formulations. After 24 h, cells were irradiated as indicated above and then incubated in the presence of 10 μM DCFH-DA, as previously described [22]. After solubilizing cells with Triton X-100, DCF fluorescence was detected in a PerkinElmer LS55 Fluorometer (PerkinElmer Ltd., Beaconsfield, UK) using 488 nm excitation and 530 nm emission wavelengths. DNA content was estimated with 50 μM propidium iodide (PI) and results were expressed as the ratio between DCF and PI fluorescence.

2.8.4. Intracellular localization of different liposomal formulations of Pc9

KB cells grown on coverslips were incubated with 2 μM Pc9 incorporated into S and S-PEG liposomes for 24 h at 37 °C in the dark. After washing with PBS, cells were stained with LysoTracker Green DND-26 (75 nM, 30 min) and MitoTracker Green FM (100 nM, 45 min), as described previously [14,22]. Coverslips were fixed for 10 min at room temperature with 4% paraformaldehyde and cells were then examined by fluorescence with a confocal microscopy Olympus FV 300. Pc9 was excited at 635 nm and the emission was monitored at wavelengths between 655 and 755 nm. Organelles (lysosomes and mitochondria) were excited at 473 nm and green fluorescence was detected at 485–545 nm. Cell nuclei were stained with Hoechst, excited at 405 nm and detected at 425–460 nm.

3. Results and discussion

3.1. Determination of incorporation efficiency (IE)

Pc9 was incorporated into liposomes as described in the Methods section. The IE of the Pc9 incorporated into liposomes, determined by UV/Vis spectroscopy, reached between 74.7% and 92.5% in all studied formulations (Table 1), a value higher than those recently published for other zinc(II)phthalocyanines [13].

3.2. Spectroscopic studies

The spectroscopic characterization of the absorption and emission spectra of free and incorporated Pc9 was used to establish the incorporation of the dye into liposomal formulations. Fig. 2 shows the incorporation of Pc9 in homogeneous media (THF) and into

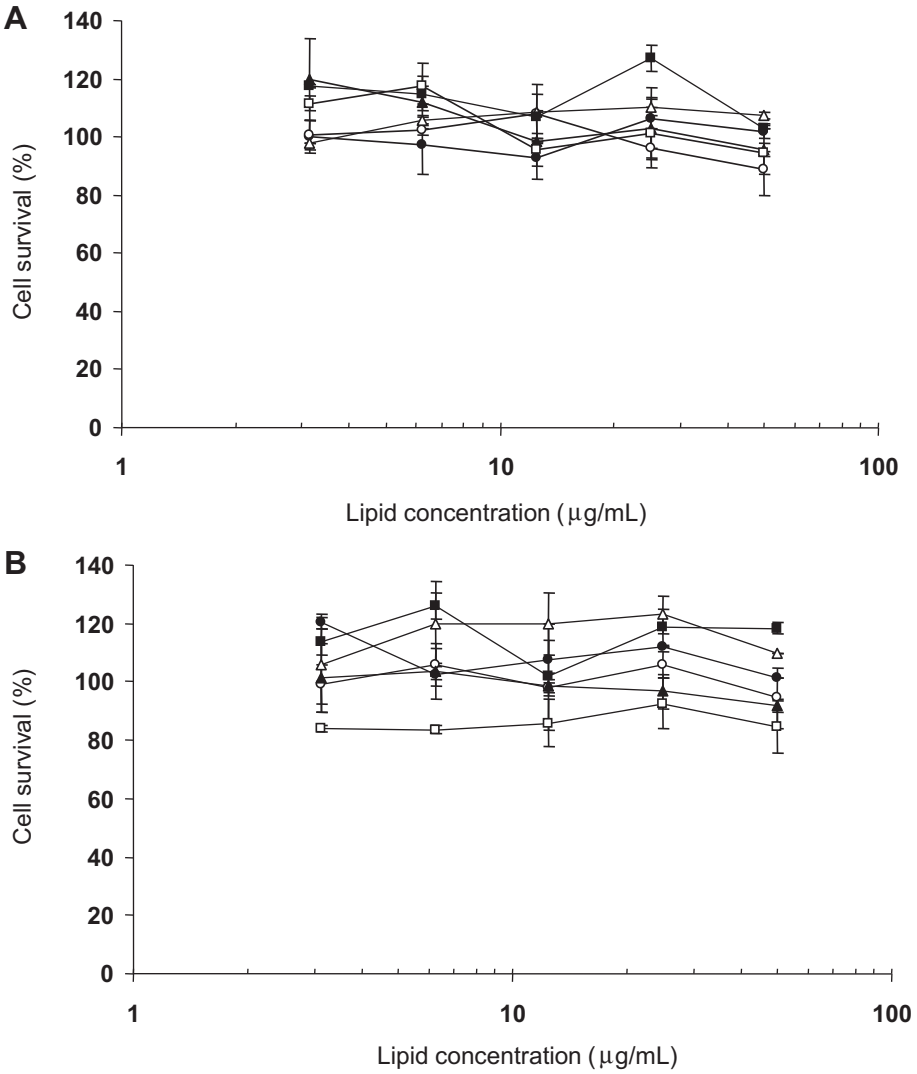

Fig. 7. Effect of different liposomes on KB cell viability. Different concentrations of the liposomes D1 (●), D2 (○), M1 (▲), M2 (△), S (■) and S-PEG (□) were incubated with KB cells in the dark (A) or exposed to a light dose of 2.8 J cm^{-2} (B). The MTT cytotoxicity assay was carried out 24 h after the treatment, as described under Materials and methods. Results are expressed as the percentage of cell growth obtained in the absence of liposome (control) and represent the mean ± S.E. of three different experiments.

liposomes. The shape of Pc9 spectra in liposomes was the same as that of other zinc(II) phthalocyanines in organic solvents and liposomes. The spectra in Fig. 2 show a wider Q-band and a new band in the range of 642–657 nm, for dimer/oligomer Pc9 (Table 2). The shape of the spectra in M2, S and S-PEG liposomes presents an intermediate behavior between hydrophilic and lipophilic media [16,23]. On the other hand, the intensities of M1, D1 and D2 dimer/oligomer peaks are higher than that of the monomeric one.

Fig. 3 shows the fluorescence spectra of Pc9 in solution (THF) and in the presence of liposomes. Neither significant wavelength shifts nor relevant modifications in shape were observed. This evidences that only the monomer is the emitting species.

3.3. Aggregation studies of Pc9 in liposomal formulations

The intensity absorption rates values observed in liposomes were higher than those observed in HEPES (0.53), but lower than those obtained in THF (6.09). The M2 liposome formulation (1.55) showed the lowest aggregation behavior, whereas M1 showed the highest one (0.76) (Table 2).

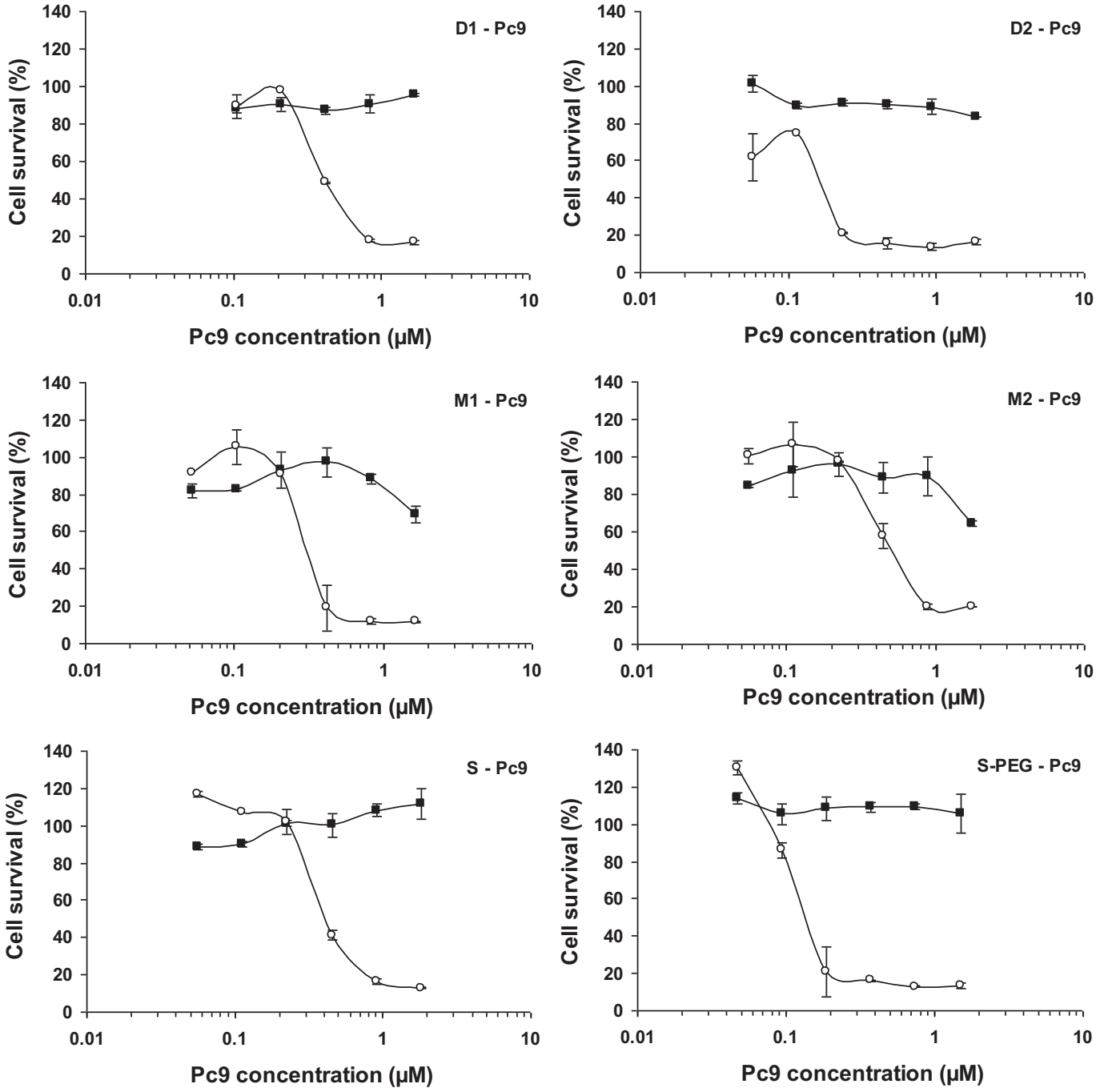

Fig. 8. Effect of Pc9 included in different liposomes on KB cell viability. Different concentrations of Pc9 were incubated with KB cells in the dark (●) or exposed to a light dose of 2.8 J cm^{-2} (○). After 24 h of incubation, cytotoxicity was assessed by the MTT assay, as described under Materials and methods. Results are expressed as the percentage of cell growth obtained in the absence of phthalocyanine-liposome (control) and represent the mean ± S.E. of three different experiments.

Table 4
IC_{50} values obtained for Pc9-loaded liposomes in KB cells.

Liposome	D1	D2	M1	M2	S	S-PEG
IC50 (μM)	0.47 ± 0.10^{a}	0.21 ± 0.07^{b}	0.30 ± 0.01^{ab}	0.40 ± 0.01^{ab}	0.40 ± 0.07^{ab}	0.21 ± 0.12^{b}

IC_{50} represent mean values ± S.E. from three determinations. Statistical analysis was performed by Tukey's test after one-way ANOVA. Different letters denote significant difference at $p < 0.05$.

3.4. Fluorescence and singlet molecular oxygen quantum yields

The Φ_F and Φ_Δ values in homogeneous and microheterogeneous media are listed in Table 2. The Φ_Δ values were calculated against MB as a reference incorporated into different liposomal formulations at a concentration where only the monomer is present (0.1 μM). In all the experiments, samples were prepared with HEPES pH = 7.4 instead of Milli-Q water. The Pc9-loaded liposomes Φ_Δ values were calculated using MB as a reference in HEPES. The Φ_Δ values were good enough to consider all formulations studied as potential agents for photodynamic purposes. In addition, they were higher than those obtained with other zinc(II) phthalocyanines incorporated into DMPC liposomes [5,13].

3.5. Determination of Pc9 solubility in liposomes

The solubility of Pc9 in water:DMSO (98:2) and formulations D1, D2, M1, M2, S, and S-PEG was studied by fluorescence and the concentrations were monitored over 1 month (Fig. 4). The intrinsic solubility in water:DMSO (98:2), D1, D2, M1, M2, S, and S-PEG was 0.48, 1.06, 1.32, 1.09, 1.07, 1.11, 1.05 respectively. A two-fold increase in solubility was observed for Pc9-loaded liposomes in comparison with water:DMSO (98:2).

3.6. Determination of binding constants

The K_a was calculated according to equation (2) for all the liposomal formulations. The values obtained are shown in Table 3 and the fitted data in Fig. 5. The S-PEG K_a value was up to six times higher than those obtained for non-stealth liposomes. This could be attributed to the tighter binding of Pc9 to the membrane of the S-PEG formulation, suggesting that the dye cannot be only between the layers, but also between the PEG tails.

3.7. Photocytotoxicity studies

The effect of different concentrations of Pc9 dissolved in 0.4% dimethyl sulfoxide (DMSO) was examined on KB cells. Survival was evaluated in the dark and upon exposure to the same light dose described below by using the MTT assay (Fig. 6) [22]. The IC_{50} value from three different independent experiments (mean ± S.E.) was 0.12 ± 0.070 μM.

To study the photocytotoxic effect of Pc9 incorporated into different liposomal formulations, the effect of empty liposomes on cell viability was first examined. As shown in Fig. 7A, after incubating KB cells in the dark with different concentrations of non-loaded liposomes, cell survival remained invariable up to lipid concentrations of 50 μg/mL. A similar behavior was observed for the six formulations tested in the presence of light (Fig. 7B). Then, the cytotoxic effect of distinct concentrations of Pc9-loaded liposomes was evaluated in KB cells both in the dark and upon exposure to a light dose of 2.8 J cm^{-2}, 1.17 mW cm^{-2}. The Pc9 incorporated into liposomes was found to be cytotoxic mainly after irradiation (Fig. 8). However, a slight dark toxicity was observed for M1 and M2 liposome formulations loaded with the higher concentration of Pc9 tested. The IC_{50} values, obtained from these dose–response curves, are shown in Table 4. Although similar cytotoxic effects were observed for the different Pc9 liposome formulations, S-PEG and D2 seem to be the most effective, indicating that photodynamic activity of zinc(II) phthalocyanines in tumor cells is dependent on liposomal formulation [9,24]. An increase of the photodynamic activity has also been reported for other photosensitizers incorporated into different carriers [25–28].

3.8. Intracellular production of reactive oxygen species

The ability of the Pc9 liposomal formulations to generate ROS, which finally leads to oxidative damage and cell death, was evaluated. After irradiation of KB cells pre-treated with Pc9-loaded liposomes, the production of ROS was detected with the probe DCFH-DA, which is oxidized in the presence of ROS to the fluorescent 2′,7′-dichlorofluorescein (DCF). As shown in Fig. 9, a significant increase in ROS levels was observed for all the liposomes tested. However, the statistical analyses of these results showed a significant distinction between S-PEG or D2 and S, belonging the first two preparations to the group of more cytotoxic Pc9-loaded liposomes. Taking into account the photophysical and photobiological properties or Pc9-loaded liposomes, intracellular localization studies were further performed with S and S-PEG formulations to analyze the influence of PEGylation in the cellular localization.

3.9. Intracellular localization of Pc9 incorporated into S and S-PEG liposomes

The subcellular localization of Pc9 loaded into S and S-PEG liposomes was evaluated by confocal microscopy. KB cells were incubated for 24 h in the dark and then stained with fluorescent dyes for lysosomes (LysoTracker Green), mitochondria (MitoTracker Green) or nuclei (Hoechst). Similar fluorescent images were observed for Pc9 irrespective of the liposomal formulation

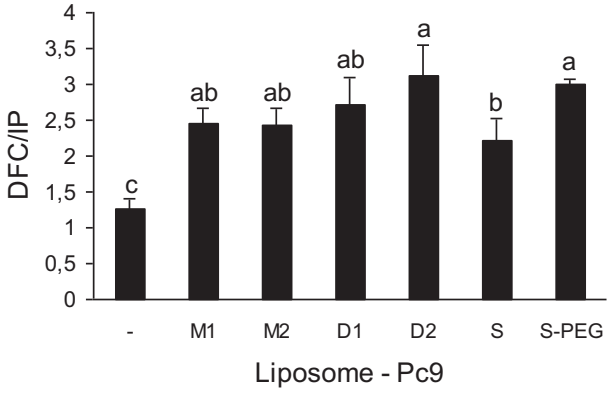

Fig. 9. Effect of Pc9 loaded on different liposomes on ROS generation in KB cells. KB cells (6×10^4 cells/well), pre-loaded with 1 μM of Pc9, were irradiated and then incubated at 37 °C for 30 min in the presence of 10 mM DCFH-DA. After washing the non-incorporated probe, cells were solubilized and DCF fluorescence was measured in a fluorometer. DNA content was estimated after incubating with a final concentration of 50 μM PI in the dark. Results are expressed as the ratio between DCF and PI fluorescence, and represent the mean ± S.E. of three different experiments. Statistical significance, obtained by Bonferroni after one-way ANOVA, was $p < 0.05$.

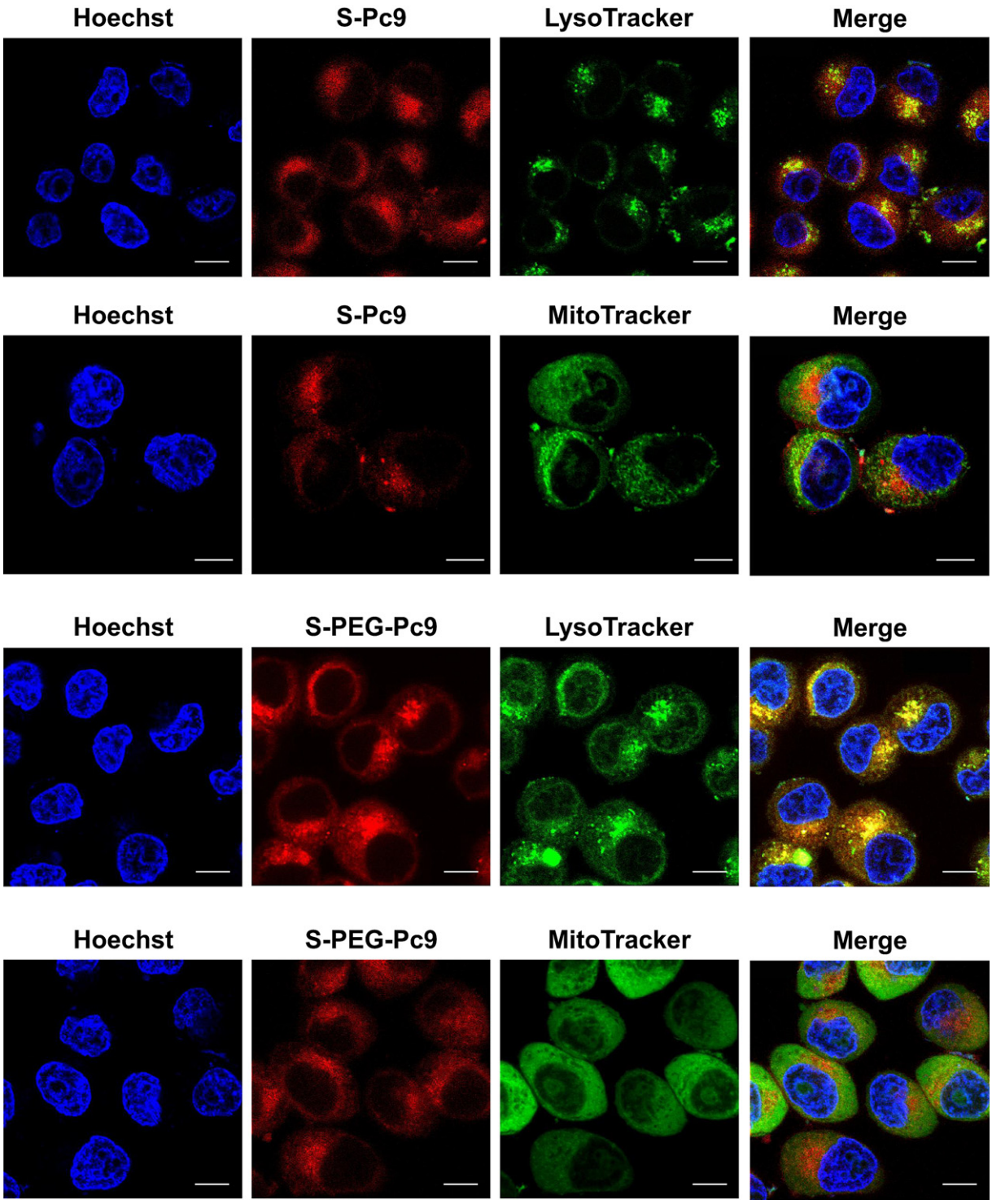

Fig. 10. Intracellular localization of Pc9. KB cells incubated for 24 h with 2 μM of Pc9 loaded into S or S-PEG liposome were stained with LysoTracker Green DND-26 (75 nM, 30 min) or MitoTracker Green FM (100 nM, 45 min). Overlays of the red fluorescence corresponding to Pc9 and the green fluorescence signal for lysosomes and mitochondria are shown. Cell nuclei were visualized with Hoechst dye. Magnification × 2430, scale bar 10 μm. (For interpretation of the references to color in this figure legend, the reader is referred to the web version of this article.)

used. Thus, a typical red fluorescence emission of Pc9 revealed a cytosolic localization of the phthalocyanine incorporated either to S or S-PEG liposomes (Fig. 10). In addition, Pc9 was found mainly within cytosolic vesicles corresponding to lysosomes, as a yellow fluorescence signal visualized from the overlay of the red fluorescence from Pc9-S or Pc9-S-PEG liposomes and the LysoTracker Green probe. No evident colocalization was detected for Pc9 within mitochondria, remaining the green punctuate pattern of MitoTracker Green separate from the red fluorescence of Pc9 (Fig. 10). Preferential lysosome localization has also been reported for other metallophthalocyanines incorporated into liposomes [6].

4. Conclusions

The absorption spectra of Pc9 incorporated into different liposomal formulations showed a red spectral shift as compared with those in homogeneous media. This bathochromic shift could improve skin light penetration and be useful for clinical purposes. As shown in Fig. 2 for all formulations, a wider Q-band and a new band between 640 and 650 nm for dimer/oligomer Pc9 were obtained. For M2, S, and S-PEG, the monomer peak was higher than the dimer/oligomer one, while M1, D1 and D2 showed a higher dimer/oligomer peak.

Fluorescence spectra also showed a red spectral shift as compared with those in homogeneous media. Pc9 liposomal formulations are efficient singlet oxygen quantum yield generators. The Φ_Δ values were good enough to consider all formulations studied as potential agents for photodynamic purposes.

The solubility of Pc9 was improved by the incorporation into the different formulations studied as compared with the solubility of the dye in water:DMSO. Besides, the aggregation in all liposome formulations was lower than that in buffer HEPES.

The affinity of Pc9 in the S-PEG formulation was the highest.

The in vitro photodynamic activity was evaluated on human nasopharynx KB carcinoma cells. In the concentration range studied, D1, D2, M1, M2, S, and S-PEG were non-toxic carriers. None of the Pc9 formulations showed dark toxicity up to a 1 μM Pc9 concentration. A potent cytotoxic effect was evident after irradiation, being IC_{50} values between 0.21 and 0.47 μM Pc9 for the different liposomes tested.

A lysosomal localization was found for S-PEG as well as for S.

Our previous studies showed that the mean diameter of S and S-PEG was 80.9 and 207.1 nm respectively [13]. Therefore, we assume that pinocytosis is the probable uptake mechanism, since it can be conducted by virtually all cell types and normally involves ingestion of sub-micron material and substances in solution [29]. Studies of Pc9 delivery to its site to action are actually in progress.

The above results have prompted us to consider performing in vivo studies of Pc9 incorporated into S-PEG.

Acknowledgments

This work was supported by grants from the University of Buenos Aires (X-063), the Consejo Nacional de Investigaciones Científicas y Técnicas (CONICET, PIP 104) and the Agencia Nacional de Promoción Científica y Tecnológica (PICT 1030). Argentina. The assistance of Ms Victoria Eusevi in language supervision is appreciated.

References

[1] MacDonald IJ, Dougherty TJ. Basic principles of photodynamic therapy. J Porphyr Phthalocyanines 2001;5:105–29.
[2] Kudinova NV, Berezov TT. Photodynamic therapy of cancer: search for ideal photosensitizer. Biochem (Moscow) Supple Ser B Biomed Chem 2010;4:95–103.
[3] Allen CM, Sharman WM, van Lier JE. Current status of phthalocyanines in the photodynamic therapy of cancer. J Porphyrins Phthalocyanines 2001;5:161–9.
[4] Kaestner L, Cesson M, Kassah K, Christensen T, Edminson PD, Cook MJ, et al. Zinc octa-n-alkyl phthalocyanines in photodynamic therapy: photophysical properties, accumulation and apoptosis in cell cultures, studies in erythrocytes and topical application to Balb/c mice skin. Photochem Photobiol Sci 2003;2:660–7.
[5] Rodriguez ME, Moran F, Bonansea A, Monetti M, Fernández DA, Strassert CA, et al. A comparative study of photophysical and phototoxic properties of octakis(decyloxy)phthalocyaninato zinc (II), incorporated in a hydrophilic polymer, in liposomes and in non ionic micelles. Photochem Photobiol Sci 2003;2:988–94.
[6] Rodriguez ME, Zhang P, Azizuddin K, Delos Santos GB, Chiu S, Xue L, et al. Structural factors and mechanisms underlying the improved photodynamic cell killing with silicon phthalocyanine photosensitizers directed to lysosomes versus mitochondria. Photochem Photobiol 2009;85:1189–200.
[7] Derycke ASL, Witte PAM. Liposomes for photodynamic therapy. Adv Drug Deliv Rev 2004;56:17–30.
[8] Nunes SMT, Sguilla FS, Tedesco AC. Photophysical studies of zinc phthalocyanine and chloroaluminum phthalocyanine incorporated into liposomes in the presence of additives. Braz J Med Biol Res 2004;37:273–84 [and references therein].
[9] Rumie Vittar NB, Prucca CG, Strassert CA, Awruch J, Rivarola VA. Cellular inactivation and antitumor efficacy of a new zinc phthalocyanine with potential use in photodynamic therapy. Int J Biochem Cell Biol 2008;40:2192–205.
[10] Rodriguez ME, Awruch J, Dicelio LE. Photophysical properties of Zn(II) phthalocyanines into liposomes. J Porphyrins Phthalocyanines 2002;6:122–9.
[11] Torchilin V. Multifunctional carriers. Adv Drug Deliv Rev 2006;58:1532–55.
[12] Diz VE, Gauna GA, Strassert CA, Awruch J, Dicelio LE. Photophysical properties of microencapsulated photosensitizers. J Porphyrins Phthalocyanines 2010;14:278–83.
[13] López Zeballos NC, García Vior MC, Awruch J, Dicelio LE. An exhaustive study of a novel sulfur-linked adamantane tetrasusbtituted zinc(II) phthalocyanine incorporated into liposomes. J Photochem Photobiol A Chem 2012;235:7–13.
[14] Marino J, Garcia Vior MC, Dicelio LE, Roguin LP, Awruch J. Photodynamic effects of isosteric water-soluble phthalocyanines on human nasopharynx KB carcinoma cells. Eur J Med Chem 2010;45:4129–39.
[15] Fernández DA, Awruch J, Dicelio LE. Photophysical and aggregation studies of *t*-butyl substituted Zn phthalocyanines. Photochem Photobiol 1996;63:784–92.
[16] Wilkinson F, Helman WP, Rose AD. Rate constant for the decay and reactions of the lowest electronically excited singlet state of molecular oxygen in solution. J Phys Chem Ref Data 1995;24:663–1021.
[17] Kraljic I, El Mohsni S. A new method for the detection of singlet oxygen in aqueous solution. Photochem Photobiol 1978;28:577–81.
[18] Amore S, Lagorio MG, Dicelio LE, San Román E. Photophysical properties of supported dyes. Quantum yield calculations in scattering media. Prog React Kinet Mech 2001;26:159–77.
[19] Alarcón E, Edwards AM, Garcia AM, Muñoz M, Aspée A, Borsarelli CD, et al. Photophysics and photochemistry of zinc phthalocyanine/bovine serum albumin adducts. Photochem Photobiol Sci 2009;8:255–63.
[20] Rodríguez ME, Fernández DA, Awruch J, Braslavsky SE, Dicelio LE. Effect of aggregation of a cationic phthalocyanine in micelles and in the presence of human serum albumin. J Porphyrins Phthalocyanines 2006;10:33–42.
[21] García Vior MC, Monteagudo E, Dicelio LE, Awruch J. A comparative study of a novel lipophilic phthalocyanine incorporated into nanoemulsion formulations: photophysics, size, solubility and thermodynamic stability. Dyes Pigment 2011;91:208–14.
[22] Gauna GA, Marino J, García Vior MC, Roguin LP, Awruch J. Synthesis and comparative photodynamic properties of two isosteric alkyl substituted zinc(II) phthalocyanines. Eur J Med Chem 2011;46:5532–9.
[23] Sharman WM, Allen CM, van Lier JE. Photodynamic therapeutics: basic principles and clinical applications. Drug Discov Today 1999;4:507–17.
[24] García AM, Alarcón E, Muñoz M, Scaiano JC, Edwards AM, Lissi E. Photophysical behaviour and photodynamic activity of zinc phthalocyanines associated to liposomes. Photochem Photobiol Sci 2011;10:507–14.
[25] Alléman E, Rousseau M, Brasseurs N, Kudrevich SV, Lewis K, van Lier JE. Photodynamic therapy of tumour with hexadecafluoro zinc phthalocyanine formulated in PEG-coated poly(lactic acid) nanoparticles. Int J Cancer 1996;66:821–4.
[26] Konan YN, Gurny R, Allémann E. State of the art in the delivery of photosensitizers for photodynamic therapy. J Photochem Photobiol B Biol 2002;66:89–106.
[27] Konan YN, Berton M, Gurny R, Allémann E. Enhanced photodynamic activity of meso-tetra(4-hydroxyphenyl)porphyrin by incorporation into sub-200 nm nanoparticles. Eur J Pharm Sci 2003;18:241–9.
[28] Postigo F, Mora M, De Madariaga MA, Nonell S, Sagristá ML. Incorporation of hydrophobic porphyrins into liposomes: characterization and structural requirements. Int J Pharm 2004;278:239–54.
[29] Faraji AH, Wipf P. Nanoparticles in cellular drug delivery. Biorg Med Chem 2009;17:2950–62.